

Electron Capture into the $n = 3$ States of H by Fast H^+ Impact on N_2^+

R. H. Hughes, B. M. Doughty,* and A. R. Filippelli

Department of Physics, University of Arkansas, Fayetteville, Arkansas

(Received 26 March 1968)

Electron capture into the $3s$, $3p$, and $3d$ states of hydrogen has been measured for 10–35 keV proton impact on N_2 . Polarization of the $3d \rightarrow 2p$ and $3p \rightarrow 2s$ radiations resulting from the collisions has also been measured. The cross sections for the production of Balmer-alpha radiation have been calculated from the $3s$, $3p$, and $3d$ cross sections and compared with those of previous investigations. The $3d$ cross section is about equal to the $3s$ cross section at 10 keV, but decreases monotonically as the energy is increased to 35 keV.

I. INTRODUCTION

A prior publication¹ described a time-of-flight technique which permitted the measurement of the cross section for electron capture into the $3s$ state resulting from proton impact on several gases. In these experiments fast protons entered a differentially pumped collision chamber, containing the target gas, where electron capture took place. The partially neutralized beam then entered an evacuated observation chamber. Capture into the $n = 3$ level of hydrogen was monitored by observing the Balmer-alpha ($n = 3 - 2$) radiation in the observation chamber. It was shown that the decay of Balmer-alpha radiation along the beam could be resolved into $3p$, $3d$, and $3s$ decays with the proper theoretical lifetimes^{1,2} when the "background" from the interaction of the beam with the residual gas in the observation chamber was taken into account.

Capture into the $3s$ state¹ and $4s$ state³ has been measured by monitoring the Balmer-alpha and Balmer-beta emissions, respectively, at a point in the observation chamber sufficiently distant from the exit aperture so that all the shorter-lived states contributing to these emissions have decayed off. In the low-pressure approximation, neglecting cascade, the excited-atom density is given by

$$n^* = n_0^+ e^{-x/v\tau},$$

where x is the distance from the exit aperture, v is the atom velocity, τ is the state lifetime, $n_0^+ = F\rho Q\tau(1 - e^{-L/v\tau})$ and is the excited hydrogen atom density at $x = 0$, F is the proton flux, ρ is the collision-chamber gas density, Q is the cross section for capture into the state, and L is the length of the collision chamber.

The general expression for the number of Balmer-alpha photons per sec per cm^3 emanating from a point x in the observation chamber is given by

$$N = n_p^0 A_p e^{-x/v\tau_p} + n_d^0 A_d e^{-x/v\tau_d} + n_s^0 A_s e^{-x/v\tau_s}, \quad (1)$$

where A_p , A_d , and A_s are the $3p \rightarrow 2s$, $3d \rightarrow 2p$, and $3s \rightarrow 2p$ transition probabilities, respectively; the n^0 's and τ 's carry subscripts to indicate the p , d , or s states. The lifetimes of the three states are very different, which allows the breakdown of the Balmer-alpha emission as a function of x into

its three decay modes.² From this analysis, the n_p^0 , n_d^0 , and n_s^0 can be determined, and these in turn determine the p , d , and s cross sections; Q_p , Q_d , and Q_s ; respectively.² However, previous attempts to include the $3p$ and $3d$ measurements have been unsuccessful.¹ In this paper we report the successful measurement of capture into the $3p$ and $3d$ states of hydrogen from proton impact on N_2 . In Sec. II we derive general expressions for the buildup of excited atoms in the collision chamber.

II. BUILDUP OF FAST EXCITED ATOMS

We consider now the production and loss of beam atoms in a particular excited state at a point y in the collision chamber where y is the distance from the entrance aperture measured along the beam direction. It is assumed that the charge state of the beam at y is governed principally by charge transfer and stripping (collisional ionization). The density of protons at y is given by

$$n_+ = \frac{n_+^0}{\sigma_s + \sigma_c} \{ \sigma_s + \sigma_c \exp[-\rho(\sigma_s + \sigma_c)y] \}, \quad (2)$$

where n_+^0 is the entering-proton density at $y = 0$, σ_s is the total stripping cross section, σ_c is the total charge-transfer cross section, and ρ is the gas density. The density of neutrals at y is given by

$$n_0 = \frac{n_+^0}{\sigma_s + \sigma_c} \sigma_c \{ 1 - \exp[-\rho(\sigma_s + \sigma_c)y] \}. \quad (3)$$

The rate equation at y governing the density of excited atoms, n^* , is

$$dn^*/dy = -n^*(1/v\tau + Q_i\rho) + n_+\rho Q + n_0 Q_x \rho, \quad (4)$$

where v is the velocity, τ is the state lifetime, Q is the cross section for electron capture into the state, Q_i is the cross section for collisional loss of the state, Q_x is the cross section for producing the state by neutral collisional excitation, n_+ is the proton density, and n_0 is the hydrogen atom density.

The solution to Eq. (4), using Eqs. (2) and (3), is

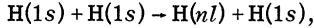
$$n^* = \frac{n_+^0 \rho y}{\sigma_s + \sigma_c} \frac{\sigma_s Q + \sigma_c Q_x}{y/v\tau + \alpha} [1 - \exp(-y/v\tau - \alpha)] + \frac{\sigma_c (Q - Q_x) [\exp(-\beta - \gamma) - \exp(-y/v\tau - \alpha)]}{y/v\tau - (\beta + \gamma) + \alpha}, \quad (5)$$

where $\alpha = \rho y Q_i$, $\beta = \rho y \sigma_c$, and $\gamma = \rho y \sigma_s$. For sufficiently low pressures, we can expand about $\alpha = \beta + \gamma = 0$ and evaluate Eq. (5) at $y = L$ to obtain the excited-state density at the exit aperture of a collision chamber having a length L . If all second- and higher-order terms are negligible, the result of the expansion can conveniently be expressed as

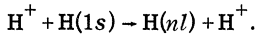
$$n^* = n_+ e^{\rho v \tau Q (1 - e^{-L/v\tau})} \times [1 - (1-a)\alpha + a(Q_x/Q)\beta], \quad (6)$$

where $\alpha = \rho L Q_i$, $\beta = \rho L \sigma_c$, $a = [1 - e^{-L/v\tau}]^{-1} - (L/v\tau)^{-1}$, and $n_+ e^{\rho v \tau Q (1 - a\beta)}$ is the "effective" proton density. [The measured proton density at the exit aperture is $n_+^m = n_+^0 (1 - \beta)$.] If $L/v\tau \approx 0$ for a very long-lived state, $a \approx \frac{1}{2}$; and if $L/v\tau \approx \infty$ for a very short-lived state, $a \approx 1$. Thus, $\frac{1}{2} < a < 1$ for all states. Ignoring the last two terms in Eq. (6), one sees that the average proton density in the chamber should be used in making beam-attenuation corrections for a long-lived state, while essentially no correction should be employed for short-lived states. However, it is not obvious that these last two terms should be ignored.

Bates and Walker⁴ suggest that the cross section for stripping from an $n = 3$ state of hydrogen for hydrogen atom impact on N_2 is $\sim 10^{-15}$ cm² in this energy range. This large cross section implies that $Q_i \sim \sigma_c$ or $\alpha \sim \beta$. The "excitation" term, $a Q_x \beta / Q$, depends on the probability of exciting a hydrogen atom to the state by impact. Bates and Griffing⁵ have calculated the cross section Q_x for



and Bates and Dalgarno⁶ have calculated the cross section Q for



A comparison of these two works reveals that for $n = 3$ at 10 keV, $Q_x/Q \sim \frac{1}{10}$. However, the validity of the Born approximation at this energy can be questioned.

Our work so far has not been sufficiently accurate to really test the relative size of the "collisional loss" term, $(1-a)\alpha$, and the "excitation" term, $a(Q_x/Q)\beta$. Our "linearity-with-pressure" studies seem to indicate that ignoring these terms and simply correcting for beam neutralization is sufficient. Since the correction is small, no great error should be introduced even if this procedure is not quite right. (We should point out that for the longer-lived states these last two terms in Eq. (6) tend to cancel each other, while the "collisional-loss" term tends to zero for very short-lived states.)

III. POLARIZATION CONSIDERATIONS

Polarization is defined as

$$P = (I_{\parallel} - I_{\perp}) / (I_{\parallel} + I_{\perp}),$$

where I_{\parallel} and I_{\perp} are the intensities of the radiation with the electric vector parallel to and perpendicular to the beam direction, respectively, when the viewing direction is perpendicular to the beam. When observing perpendicular to the beam, the

true cross section Q is given by

$$Q = (3-P)Q_a/3,$$

where Q_a is the apparent cross section. The 3s radiation is unpolarized, but the 3p and 3d radiations will exhibit polarization effects.

Percival and Seaton⁷ have treated polarization of radiation quite extensively. They do not, however, treat the hydrogen ${}^2D \rightarrow {}^2P$ transitions. We have derived an expression for the polarization of the $3{}^2D \rightarrow 2{}^2P$ transition. It is

$$P(3{}^2D \rightarrow 2{}^2P) = 57(Q_0 + Q_1 - 2Q_2) \times (119Q_0 + 219Q_1 + 162Q_2)^{-1}, \quad (7)$$

where Q_0 , Q_1 , and Q_2 are the cross sections for populating the $m_l = 0$, $|m_l| = 1$, and $|m_l| = 2$ states, respectively. (The cross section for populating the 2D state is $Q_d = Q_0 + 2Q_1 + 2Q_2$.) The polarization expected for the transition depends on the detailed knowledge of Q_0 , Q_1 , and Q_2 . We can, however, put limits on it. If the linear-momentum transfer is all along the axis of quantization, then $Q_1 = Q_2 = 0$, but if it is perpendicular to the axis, then $Q_1 = 0$ and $Q_2 = \frac{3}{2}Q_0$ (see Ref. 7, page 133), which leads to the result

$$-0.32 < P(3{}^2D \rightarrow 2{}^2P) < +0.48.$$

Cross sections for populating m_l states by electron capture by fast protons on atomic hydrogen have been calculated by Van den Bos and de Heer⁸ for levels which include the $n = 3$ level. Using their values, a constant polarization of about +39% is expected in our energy range for the $3{}^2D \rightarrow 2{}^2P$ transition; and a constant polarization of about +33% is expected for the $3{}^2P \rightarrow 2{}^2S$ transition. As the velocity increases, limiting values of +40% and +35% are expected for the polarizations of $3{}^2D \rightarrow 3{}^2P$ and $3{}^2P \rightarrow 2{}^2S$ transitions, respectively.

IV. APPARATUS

The present apparatus is similar to that described in Ref. 1. The principal modification was the insertion of precollimation apertures. The beam is now so highly collimated that the beam particles pass through the $\frac{1}{16}$ -in. diam exit aperture with only minimum interaction with the material surrounding the exit aperture. There is no physical evidence, such as "burning" around the aperture, that the beam strikes the aperture sides.

We conclude that the precollimation of the beam has remedied the defects in the earlier apparatus which precluded the 3p and 3d measurements. One possible contributing factor is that charging around the exit aperture, which would result from the beam striking "dirty" surfaces, was reduced. Other possible contributing factors are that the motional electric field was reduced slightly by moving the collision chamber farther from the fringing field of the ion-deflecting magnet, and the space-charge electric field was reduced by the necessity of smaller currents. Lastly, precollimation has increased the accuracy of the measurements next to the aperture by eliminating part of the background which may have been related to outgassing in the vicinity of the exit aperture by ion impact.⁹

Additional modifications were employed for the

testing of possible Stark mixing. These included modifying the collision chamber so that an axial electric field could be applied in the collision chamber. In another test, a set of coils were distributed around the collision chamber so that a magnetic field could be carefully aligned parallel to the beam direction. The idea behind this latter modification was to increase the separation between the $P_{3/2}$ and $D_{3/2}$ states in order to reduce Stark mixing between these two levels, which normally are separated by an amount small compared with the radiation widths and therefore are the most sensitive of the $n=3$ states to mixing. These tests were inconclusive, however.

We cannot offer conclusive proof that our cross sections are not affected by Stark mixing. On the other hand, we have no evidence of Stark mixing. The buildup of all $n=3$ states as a function of chamber length is consistent with field-free theory, within experimental error. The largest known electric field encountered in our experiment is that produced by the motion of a fast atom in the presence of a transverse magnetic field. An atom traveling with a velocity of a 30-keV proton will encounter a transverse magnetic field of 0.2 G according to our survey. This is equivalent to an electric field of about 0.5 V/cm. The critical field for complete mixing of the $3D_{3/2}$ and $3P_{3/2}$, $m = \pm \frac{3}{2}$, states by an electric field parallel to the axis of quantization, which will induce $m = \pm \frac{3}{2} \leftrightarrow \pm \frac{3}{2}$, is 1.9 V/cm.¹⁰ The motional electric field, however, is perpendicular to the axis of quantization, which is the beam direction. A comparison of the electric-dipole matrix elements shows that the states most sensitive to this electric field direction are the $m = \pm \frac{1}{2}$ states where the field will induce $m = \pm \frac{1}{2} \leftrightarrow \mp \frac{1}{2}$. The critical field in this case is 2.9 V/cm. The amount of mixing produced by a transverse field of only 0.5 V/cm can easily be neglected, since both the lifetimes and apparent cross sections (see Fig. 3) for the $3d$ and $3p$ states only differ by at most a factor of 3. This produces a 2% or less change in either the apparent lifetimes or the apparent cross sections for the $P_{3/2}$ and $D_{3/2}$ levels.

Collision chamber lengths of 3 and 6 cm were used in the measurements, the greater number of these measurements having been performed on the 3-cm chamber. The shorter chamber has the advantage of minimizing the buildup of the $3s$ states and thus enhances the relative $3p$ and $3d$ measurements.

The previous work had been done with a mask 1 cm in length on the photomultiplier, which allowed a 1-cm length of beam to be viewed through the unit magnification optical system. The mask was reduced to $\frac{1}{2}$ cm in length for this experiment to get increased resolution in the total decay curve. A lock-in detection system was used for most of this work. Electrostatic deflection plates swept the beam off and on the axis of the collimation system at a frequency of 1 kHz.

V. PROCEDURE

The decay curves are analyzed in the conventional fashion as shown in Fig. 1. The 160-nsec $3s$ decay is first subtracted from the gross decay. The

15.6-nsec $3d$ decay is then subtracted from the remainder, leaving the 5.4-nsec $3p$ decay. The intercepts of the decay components at the exit aperture are then used to determine the capture cross sections.

It was determined that the Balmer-alpha emissions were linear with pressure and beam current when the small beam-attenuation corrections were applied, assuring that single collision events were being observed. When this fact was established, a Balmer-alpha "excitation function" for the emissions at the exit aperture was determined (Fig. 2). (The emission at the exit aperture at a constant pressure per unit current was measured as a function of energy.) The ratios of the $3s$, $3p$, and $3d$ radiations to the total Balmer-alpha radiation at the aperture were then determined from the decay curves. A relative excitation function for each separate component could then be deduced. These excitation functions were put on an absolute basis by normalizing the $3s$ excitation function to the previously determined $3s$ cross section curve of Ref. 1.

The polarization of the emitted radiation is a function of the distance along the decay curve and is given by

$$P(x) = [P_p B(x) + P_d C(x)]$$

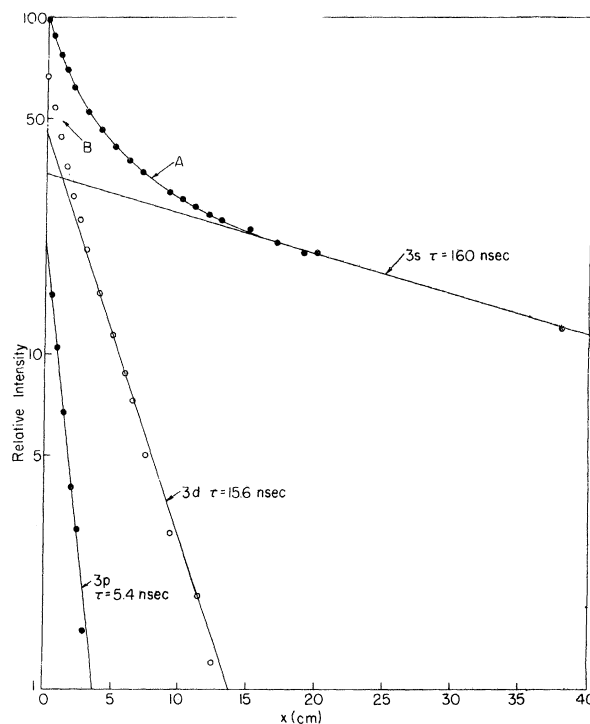


FIG. 1. Balmer-alpha decay from 27.5 keV proton impact on N_2 . The chamber length is 3 cm, the pressure is 1.1×10^{-3} Torr, and the on-cycle beam current is 0.6 μA . Curve A is the gross decay. Curve B represents the remainder produced by subtracting the $3s$ decay from Curve A. Curve $3p$ is the remainder produced by subtracting the $3d$ decay from Curve B.

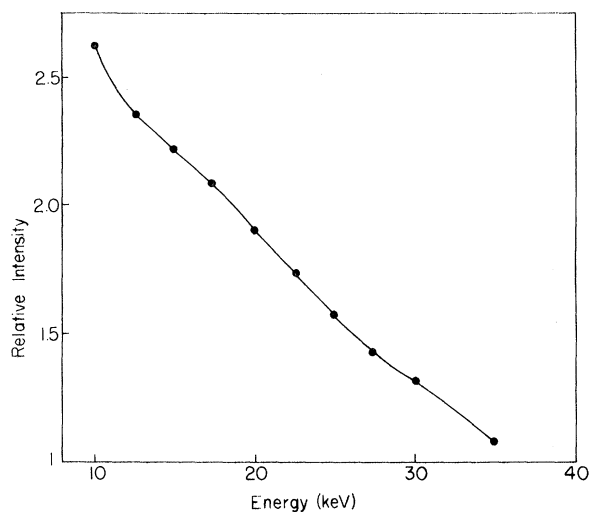


FIG. 2. Relative intensity of the Balmer-alpha radiation at the exit aperture of a 3-cm long cell containing N_2 .

$$\times [B(x) + C(x) + D(x)]^{-1}, \quad (8)$$

where $B(x) = I_p^0 \exp(-x/v\tau_p)$, $C(x) = I_d^0 \exp(-x/v\tau_d)$, $D(x) = I_s^0 \exp(-x/v\tau_s)$, and I_p^0 , I_d^0 , and I_s^0 are the intensities at the aperture ($x=0$) of the p , d , and s radiations, respectively, as measured without the polaroid analyzer; P_p and P_d are the separate polarizations of the p and d radiation, respectively. Thus, P_p and P_d can be determined uniquely by making two measurements of the polarization, substituting in Eq. (8), and solving the resulting two simultaneous equations.

VI. RESULTS AND DISCUSSION

Cross sections for electron capture into the $3p$, $3d$, and $3s$ states are displayed in Fig. 3. Reproducibilities of the $3s$ and $3d$ cross sections are about $\pm 10\%$. Reproducibility of the $3p$ cross sections for 20-keV and higher-energy impact is about $\pm 25\%$.

Reproducibility of and confidence in the $3p$ measurements drop appreciably at the lower energies. Only 12% of the $3p$ decay goes into Balmer-alpha while 100% of the $3s$ and $3d$ decays goes into this line, which accounts for the small $3p$ contribution to the total decay (see Fig. 1). At 20 keV, about 20% of the total signal at the aperture can be attributed to the $3p$ decay. Below this energy, the smaller $3p$ fractional contribution and the inherent difficulty of making measurements with smaller $v\tau$ values make the $3p$ measurements very awkward. Figure 4 is included to emphasize this point. According to this interpretation, the $3p$ decay represents about 10% of the total signal at the aperture for 15-keV impact. However, adjustments in the $3s$ and $3d$ interpretations could conceivably change the $3p$ cross section by a factor of nearly 2. Fortunately, the aperture position is well defined and can be established to within something better than ± 1 mm, and is not a limiting factor in these measurements.

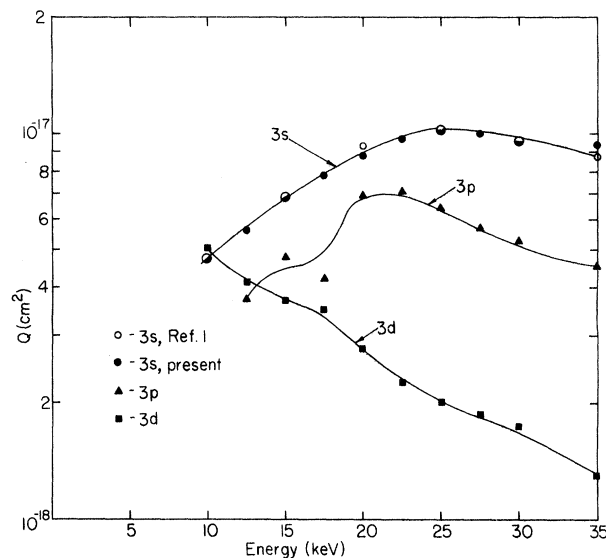


FIG. 3. Cross sections for electron capture into the $3p$, $3d$, and $3s$ states of atomic hydrogen by proton impact on N_2 . (See text regarding reproducibility and confidence in the measurements.)

The cross sections in Fig. 3 have been corrected for polarization effects. Figure 5 shows a plot of the polarization of the $3d$ radiation as determined by the application of Eq. (8) to the polarization measurements along the gross decay curve.

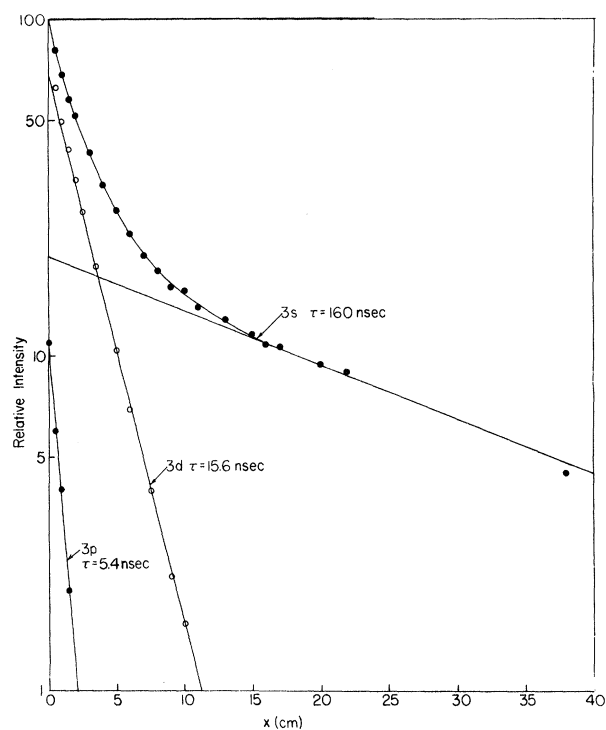


FIG. 4. Balmer-alpha decay and component decay from 15-keV proton impact on N_2 . Conditions are similar to those for Fig. 1.

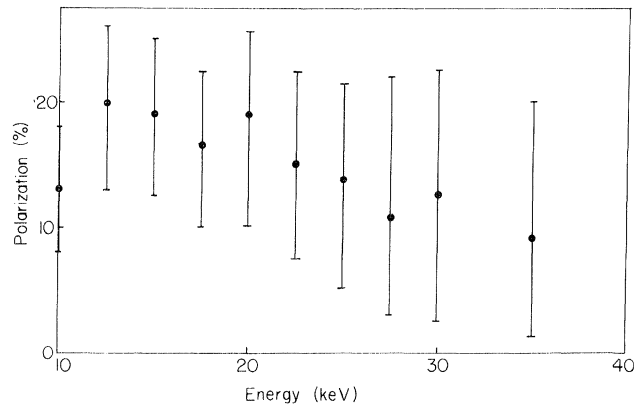


FIG. 5. Polarization of the $3^2D \rightarrow 2^2P$ transition in fast hydrogen atoms produced by proton impact on N_2 . Errors are estimated limit errors. (See text for remarks on $3^2P \rightarrow 2^2S$ polarization.)

Our results indicated that the polarization of the p -state radiation was essentially zero at the higher energies and dropped to negative values at the lower energies. However, the accuracy of these measurements is so doubtful that we do not display them.

Total Balmer-alpha cross sections have been measured by other investigators under varying experimental conditions. Murray *et al.*¹¹ (University of Alaska) have measured the total Balmer-alpha production inside a collision chamber filled with N_2 and at a point sufficiently distant from the beam entrance aperture to insure equilibrium conditions. We are able to synthesize a total Balmer-alpha cross section, Q_α , from our measurements since

$$Q_\alpha = Q_s + 0.118Q_p + Q_d. \quad (9)$$

This is plotted in Fig. 6 and compared with the

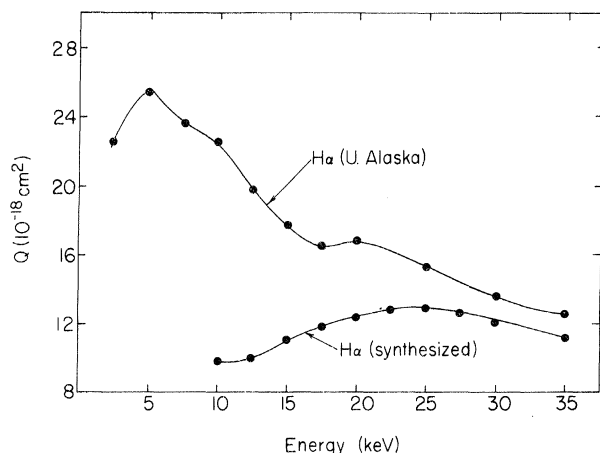


FIG. 6. Comparison of synthesized Balmer-alpha line cross section [Eq. (9)] with the total Balmer-alpha cross section measured at the University of Alaska (Ref. 11).

measurements reported in Ref. 11. There is good agreement at the high energies but our curve falls considerably below the Alaska measurements at the lower energies.

Murray *et al.*¹¹ also made polarization measurements on the Balmer-alpha radiation. We synthesized the polarization of Balmer-alpha under equilibrium conditions from our measurements and obtained results that reproduced their measurements within the reading error of their graphical display.

It is possible to synthesize an "apparent" Balmer-alpha cross section which would be measured at a point nearer the entrance aperture, where nonequilibrium conditions exist. Philpot¹² has measured the apparent cross section under such conditions in this laboratory. The midpoint of his 3-cm-long observation region was 4.7 cm from the beam entrance aperture.¹³ We can synthesize an apparent Balmer-alpha cross section under these conditions, using our cross sections. These are calculated and compared with Philpot's values¹² in Table I. (The calculated values take into account the buildup of excited states in the relatively long observation region itself; however, a good approximation can be made simply by considering the measured apparent cross section at the midpoint of the observation region.)¹⁴ The agreement is quite remarkable considering the uncertainties in both sets of cross sections. However, some agreement is to be expected if the procedures and analysis in the present experiment are valid, since the optical calibration for both experiments is derived from the same source. The agreement is gratifying and perhaps lends some credence to our present measurements.

It would appear that perhaps one probable explanation for the structure in the Balmer-alpha emission observed by Murray *et al.*¹¹ is related to the multimode decay characteristic of this line and does not have the fundamental significance suggested by these authors. However, our synthesized cross section does not reproduce their results well at the lower energies. One possibility is that there is an appreciable cascade in this total Balmer-alpha radiation since their observation was made at a point one meter from the entrance aperture, and higher long-lived states might build up in this path length. However, it seems that an excessive amount of cascade would be required to explain such a large discrepancy. We note that their measurements were not performed under single-collision conditions. The mean free path for

TABLE I. Comparison of synthesized apparent Balmer-alpha line cross section under the nonequilibrium conditions of Philpot (see Ref. 12) with the measurements of Philpot.

	Synthesized (10^{-18} cm^2)	Philpot (10^{-18} cm^2)
10 keV	5.5	5.2
15 keV	4.9	4.7
20 keV	4.4	4.0
30 keV	3.0	2.8

charge transfer is of the order of a meter at the lower energies and at their target gas pressure of "about 10^{-4} Torr." They had an appreciably mixed beam at their observation point. If their pressure was 10^{-4} Torr, then nearly 30% of the

beam would have been neutral at the 1 m point and at 10 keV.¹⁵ (The beam at this distance would have been nearly 50% neutral at 2×10^{-4} Torr and at 10 keV.) It is difficult to fully assess the effects that collisions had on their results (see Sec. II).

†Supported by the National Science Foundation.

*NASA predoctoral trainee.

¹R. H. Hughes, H. R. Dawson, B. M. Doughty, D. B. Kay, and C. A. Stigers, *Phys. Rev.* **146**, 53 (1966).

²R. H. Hughes, H. R. Dawson, and B. M. Doughty, *J. Opt. Soc. Am.* **56**, 830 (1966).

³R. H. Hughes, H. R. Dawson, and B. M. Doughty, *Phys. Rev.* **164**, 166 (1967).

⁴D. R. Bates and J. C. G. Walker, *Planetary Space Sci.* **14**, 1367 (1966).

⁵D. R. Bates and G. Griffing, *Proc. Phys. Soc. (London)* **A66**, 961 (1953).

⁶D. R. Bates and A. Dalgarno, *Proc. Phys. Soc. (London)* **A66**, 972 (1953).

⁷I. C. Percival and M. J. Seaton, *Phil. Trans. Roy. Soc. London* **A251**, 113 (1958).

⁸J. Van den Bos and F. J. de Heer, *Physica* **34**, 358 (1967). Their expressions and tabulated values for the polarization are not correct. This conclusion is confirmed by R. K. L. L. Van den Eynde, FOM Institute

for Atomic and Molecular Physics, Amsterdam, who has also obtained our Eq. (7) independently (private communication).

⁹R. H. Hughes, D. B. Kay, C. A. Stigers, and E. D. Stokes, *Phys. Rev.* **167**, 26 (1968).

¹⁰H. E. Bethe and E. E. Salpeter, *Quantum Mechanics of One- and Two-Electron Systems* (Academic Press Inc., New York, 1957), p. 288.

¹¹J. S. Murray, S. J. Young, and J. R. Sheridan, *Phys. Rev. Letters* **16**, 439 (1966).

¹²J. L. Philpot and R. H. Hughes, *Phys. Rev.* **133**, A107 (1964).

¹³J. L. Philpot, Ph.D. dissertation, University of Arkansas, 1965 (unpublished).

¹⁴J. G. Dodd, Ph.D. dissertation, University of Arkansas, 1965 (unpublished).

¹⁵Calculated by substituting the total stripping and charge-transfer cross sections tabulated by Allison [S. K. Allison, *Rev. Mod. Phys.* **30**, 1137 (1958)] into Eq. (3).

Measured Shifts of Cesium Atomic Lines — Correlation with Electron Density Derived from Widths*

R. F. Majkowski and R. J. Donohue

*Research Laboratories, General Motors Corporation,
Warren, Michigan*

(Received 12 April 1968)

The shifts of lines of the sharp, diffuse, and fundamental series of atomic cesium were measured for an rf electrodeless discharge in which the electron density was varied from 0.5 to 3×10^{14} cm^{-3} with a temperature range from 2600 to 3100°K. The shift values, which ranged from 0.008 to 1.4 Å, agree to $\pm 20\%$ with the theoretical Stark-broadening predictions for the 6P-10S, 6P-11S, 6P-12S sharp-series members; 6P-9D, 6P-10D, 6P-11D diffuse-series members; and the 6D-5F, 6D-6F, 6D-7F, 6D-8F fundamental-series members. The measured shifts exhibit a definite trend with quantum number n for all three series. At low values of n , measured shifts are greater than those computed from Stark-broadening theory, whereas measured shifts are less than theory for high n . We show that certain assumptions in the Stark-broadening theory are not applicable to most of those lines where disagreement between theory and experiment is greatest.

INTRODUCTION

The profile of a spectral line is broadened, shifted, and made asymmetric by perturbations of the energy levels of the radiating atom. For a dense plasma (say from 10^{13} – 10^{17} electrons cm^{-3}), these perturbations are caused by the electric fields (Stark effect) in the vicinity of the radiating atom. Recent theories have predicted the width and shift as a function of the electron density and temperature of the plasma.¹ Calculations of the widths of neutral atom lines are the

most reliable since they depend least on the approximations in the theory. For cesium, these widths have been accurately measured by several investigators,^{2,3,4} and are within $\pm 10\%$ of the predicted values. To test the completeness and self-consistency of the neutral line-profile theories, the complete spectral profile, i. e., the line shifts as well as shapes of cesium neutral-atom lines radiated from a plasma, were measured.

The shifts of four sharp (S) series lines, six diffuse (D) series lines, and five fundamental (F) series lines were measured at electron densities